Rapid Fabrication of Silver-Cuprous Oxide Core-Shell Nanowires for Visible Light Photocatalyst

*Siyi Yan, Qiaohui Yue, and Jiangang Ma**

Key Laboratory of UV-Emitting Materials and Technology, Ministry of Education, Northeast Normal University, Changchun, Jilin 130024, China

*majg@nenu.edu.cn (J. M.)

Experimental Section

***Preparation of Ag@Cu$_2$O NWs*:** Preparation of Ag@Cu_2O NWs includes the following steps. First, polyvinylpyrrolidone (PVP, Sigma-Aldrich) was added into the aqueous copper acetate dihydrate (Alfa Aesar) solution and then stirred. The mass concentration of Cu^{2+} was 5%. The molar concentration of PVP was in the 0–0.1 mmol/L range. Second, Ag NW ethanol solution (concentration: 0.5 mg/ml, average diameter ~80 nm, Nanjing XFNANO Materials Tech. Co., Ltd.) was added into the aqueous copper acetate solution to obtain the precursor solution. The mass concentration of Ag NWs was in the 0–0.1 mg/L range. Third, the precursor solution was irradiated with KrF excimer laser (λ = 248 nm) at room temperature in the atmospheric environment. During laser irradiation, the precursor was kept stirring at a rotation speed of 400 rpm. The duration and frequency of the pulsed laser was 20 ns and 10 Hz, the irradiation time was changed from 0–6 min. The laser energy density was 40 mJ/cm^2. The laser beam shape was rectangular with size of 2 × 2 cm^2. The fabricated Ag@Cu_2O NWs can be separated from the precursor solution by centrifugation.

***Finite-Difference Time-Domain (FDTD) Simulations*:** Commercial software package FDTD (Lumerical) was used to simulate the 2D profile of the Ag@Cu_2O nanostructures. The thickness of Cu_2O shell was in the 20–150 nm range, and the diameter of the Ag core was fixed at 50 nm. The spatial electric distribution and optical

absorption spectra excited by linearly polarized light was simulated. Bulk dielectric functions for Ag and Cu_2O were tabulated by Palik in the model. Fine FDTD mesh size of 0.5 nm was employed.

Characterization*:* The morphology observation was performed on a field emission scanning electron microscope (SEM, Hitachi S-4800). High-resolution transmission electron microscope (HRTEM) (JEOL JEM-2100F) equipped with energy dispersive X-ray spectroscopy (EDS) was used to characterize the morphologies and analyze the structure and element composition of the Ag@Cu_2O NWs. The optical absorption spectra were measured using a Hitachi UH4150 spectrometer system with an integrating sphere. X-ray diffraction (XRD) patterns were recorded on an X-ray diffractometer spectrometer (D/max 2500, Rigaku, Japan) using Cu Kα radiation (λ=1.5418 Å). Raman spectra of the Ag@Cu_2O NWs were obtained by micro-Raman spectrometer (Jobin Yvon HR800) using 488 nm He-Cd laser as excitation source.

Photocatalytic Test*:* Photocatalytic properties of the Ag NWs, the Cu_2O NPs, and the Ag@Cu_2O NWs were evaluated by the degradation of RhB under the irradiation of xenon lamp. In the photocatalytic experiment, those photocatalysts were weighed 20 mg and then dispersed into 20 ml of 10 mg/L RhB aqueous solution. The above dispersions were stirred in the dark at room temperature for 60 min to achieve an absorption-desorption equilibrium between the RhB and the photocatalyst. Then the solution was stirred and exposed to xenon lamp irradiation (300 W) with a cut off filter (λ > 400 nm). At specified intervals, approximately 2 mL of the suspension was collected and then centrifuged to remove trace impurities. The characteristic absorption of RhB at 554 nm was used to evaluate its photocatalytic degradation.

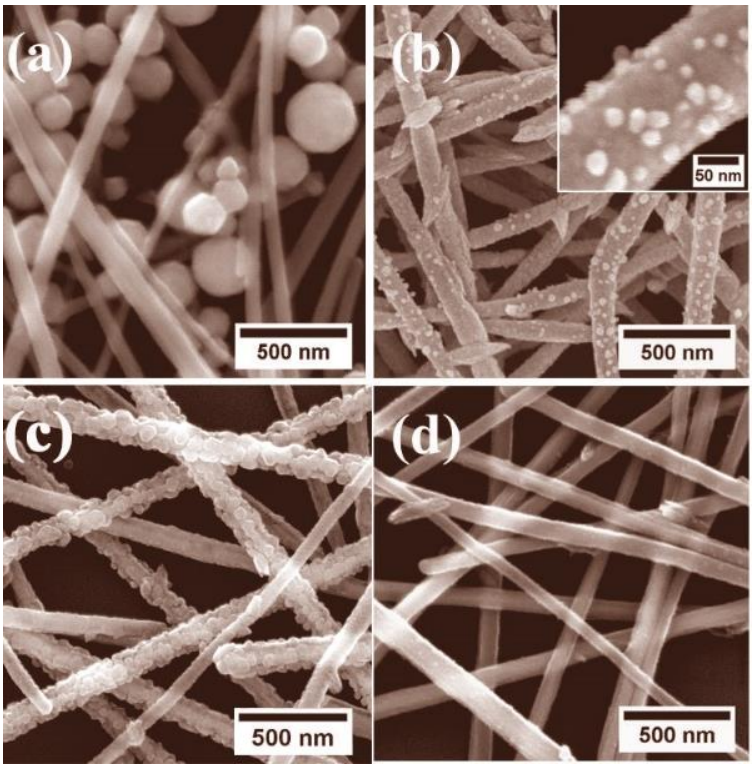

Figure S1 | Effects of Surfactant on the Morphology of Ag@Cu_2O NWs. (a–d) SEM images of Ag@Cu_2O NWs prepared at PVP molar concentration of 0, 0.5, 1, 2 mmol/L, respectively. If the PVP is not added, the Cu_2O NPs with an average size of 130 nm are produced. When the molar concentration of PVP is 0.5 mmol/L, the Cu_2O NPs with an average diameter of 100 nm are adhered on the Ag NWs. Further increasing the amount of PVP to 1 mmol/L, the average size of Cu_2O NPs decreases to 80 nm, and the Cu_2O NPs wrap on the Ag NWs densely. When the molar concentration of PVP is 2 mmol/L, the Cu_2O shell on the Ag NW surface is uniform with an average thickness of 30 nm.

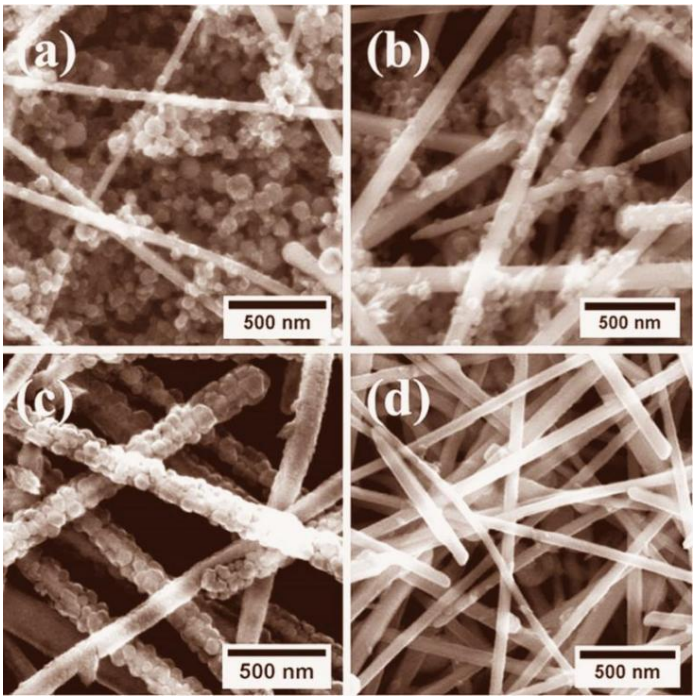

Figure S2 | Effects of Ag NWs on the Morphology of Ag@Cu_2O NWs. SEM images show the Ag@Cu_2O NWs prepared at Ag NW mass concentration of 0.025, 0.05, 0.075, and 0.1 mg/L, respectively. When the Ag NW mass concentration is 0.025 mg/L, many Cu_2O NPs are produced and a small number of them are deposited on the surface of Ag NWs. This is because the rapid reaction of copper acetate can quickly form Cu_2O nanocrystals, and the Ag NW nucleation sites are insufficient. This leads to the self-agglomeration of Cu_2O nanocrystalline. Increasing the injection amount of Ag NWs to 0.05 mg/L results in the formation of Ag@Cu_2O NWs. When the mass concentration is 0.75 mg/L, the Ag NWs are fully wrapped by Cu_2O NPs, and there are almost no free Cu_2O NPs. It indicates that the ratio of Ag NWs to Cu_2O at this time is high enough to obtain the dense and uniform Ag@Cu_2O NWs. Further increasing the mass concentration of Ag NWs to 0.1 mg/L, few Cu_2O NPs are coated on the surface of Ag NWs, and then smooth Ag@Cu_2O NWs with thin Cu_2O shells are obtained.

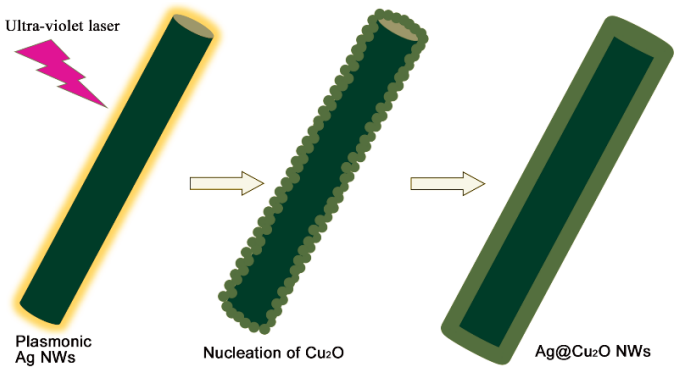

Figure S3 | Growth Mechanism of Ag@Cu$_2$O NWs. When the aqueous copper acetate solution containing Ag NWs and PVP is irradiated with ultraviolet pulsed laser, localized electric field enhancement occurs at the surface of Ag NWs due to plasmon resonance effect. This near-field enhancement promotes the following photochemical reactions to happen at the surface of Ag NWs.

$$Cu(CH_3COO)_2 \xrightarrow{h\nu} Cu(CH_3COO)_2^{*} \xrightarrow{h\nu} CH_3COOCu + CH_3COO\bullet$$

$$CH_3COO\bullet \rightarrow CH_3\bullet + CO_2\uparrow$$

$$CH_3COOCu \xrightarrow{h\nu} CH_3COOCu^{*} \rightarrow CH_3Cu + CO_2\uparrow$$

$$CH_3Cu + H_2O \rightarrow CuOH + CH_4\uparrow$$

$$2CuOH \rightarrow Cu_2O\downarrow + H_2O$$

$$2CH_3\bullet \rightarrow CH_3 - CH_3\uparrow$$

$$2Cu(CH_3COO)_2 + H_2O(l) \xrightarrow{h\nu} Cu_2O\downarrow + 4CO_2\uparrow + CH_3 - CH_3\uparrow + 2CH_4\uparrow$$

With the aid of surfactant (PVP), the Cu$_2$O tends to nucleate and grow along the surface of Ag NWs. As a result, dense and uniform Cu$_2$O will rapidly wrap on the Ag NWs to form Ag@Cu$_2$O NWs.

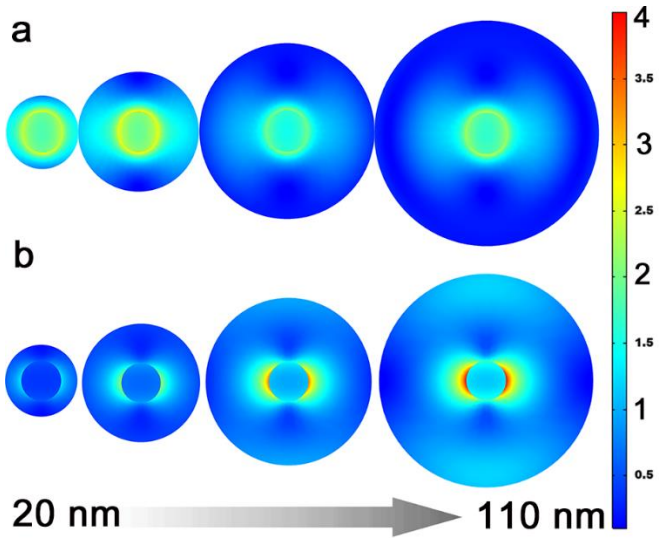

Figure S4 | FDTD-Simulated Near-Field Distributions under 400 nm (a) and 600 nm (b) excitation of the Ag@Cu_2O nanostructures. The Ag core diameter is 50 nm. The Cu_2O thicknesses are 20, 50, 80 and 110 nm.

Table S1|Comparison of photocatalytic activity of various Ag-Cu_2O composites.

Catalyst	Dye	Light Source	Degradation Efficiency (%)	Time (min)	Ref.
Ag@Cu_2O core-shell nanoparticles	methyl orange	visible light	20	120	*ACS Catal.* 2013, **3**, 47
Ag-Cu_2O nanocorncobs	methyl orange	visible light	86	150	*Mater. Research Bulletin* 2015, **70**, 296
Ag-Cu_2O core-shell nanoparticles	methyl orange	visible-light	90	300	*Catalysis Today* 2018, **303**, 313
Ag-Cu_2O composite films	methyl orange	visible light source	55	60	*J. Molecular Catalysis A: Chem.* 2013, **378**, 109
Ag-Cu_2O microcomposites	methyl orange	visible light	96	120	*Mater. Research Bulletin* 2014, **60**, 530.
Cu_2O/(Ag0@Ag-NPs)x (x = 0.0–0.25)	acid orange 7	dark	94	120	*J. Alloys Compd.* 2019, **785**, 398
Ag@Cu_2O-rGO	methyl orange	visible light	94	50	*Nanomaterials* 2018, **8**, 444
Ag@Cu_2O core-shell nanoparticles	methyl orange	visible light	81	71	*J. Colloid Interface* Sci. 2017, **486**, 16
Cu_2O-Ag composite nanospheres	methyl orange	visible-light	96	110	*Ind. Eng. Chem. Res.* 2014, **53**, 16316
Ag-Cu_2O composite octahedra	methyl orange	UV light	90	540	*Appl. Phys. A* 2014, **117**, 2189
Ag/ Cu_2O heterostructures	methylene blue	visible light	96	120	*J. Phys. Chem. Solids* 2017, **111**, 75
Ag@Cu_2O core-shell nanowires	methyl orange	UV and visible light	90	120	*ACS Appl. Mater. Interfaces* 2014, **6**, 15716
Ag@Cu_2O core-shell nanowires	rhodamine B	visible light	79	120	This work